Proceedings World Geothermal Congress 2010
Bali, Indonesia, 25-29 April 2010

Designing Thermal and Tracer Injection Backflow Tests

Ibrahim Kocabas

Chemical Engineering Dept., AUS, PO BOX 2666, Sharjah UAE

ikocabas@aus.edu

Keywords: Thermal injection-backflow tests, tracer injection-backflow tests, reinjection design, sensitivity analysis, sensible energy storage

ABSTRACT

Thermal injection backflow tests are the best method of determining heat transport parameters in geothermal and sensible energy storage reservoirs. The tracer injection backflow tests, on the other hand, are important tools for characterizing the nearby region of potential injectors.

Developing models of design and interpretation for both type of tests is of great importance for two reasons. First, the models help designing of these tests appropriately to recover maximum amount of information with minimum cost. Second, reliable estimates of parameters are of vital importance in optimal reservoir management specifically designing and operating reinjection operations.

This work presents, separate new analytical models of thermal and tracer injection backflow tests in geothermal reservoirs. Then, a parameter sensitivity analysis is applied to each model to identify the best combination of decision variables. Each combination of the decision variables are referred to as the design alternatives. The decision variables for thermal and tracer tests are, the amount of tracer to be injected, duration of injection and backflow periods and hence the distance of investigation, ratio of the injection to backflow rates, sampling domain in time (sampling interval) and frequency of sampling and finally the temperature of the injected water.

As a result, as interpretation tools, the new models provide in situ and hence, the most reliable estimates of transport parameters. As design tools, they help fixing the most desirable combination of the decision variables for the injection and backflow thermal and tracer tests. A parameter sensitivity analysis is employed to carry out the designing of both types of test. We have found that transverse tracer Peclet number and transverse thermal Peclet number are the most influential parameters. In addition, the injection to backflow ratio is effective to a lesser degree than the transverse Peclet number. The possible values of these two parameters set the best combination of decision variables.

Finally note that, the results of this work are directly applicable to assessing efficiency of sensible energy storage in aquifers as well.

1. INTRODUCTION

Reinjection may be the safest and most convenient method of disposal for heat-depleted geothermal brines. In addition, the pressure support is an important benefit of reinjection. However, premature breakthrough and injection induced cooling is a major concern associated with injection into geothermal reservoirs (Stefansson, 1997; Axelsson *et al.*, 2001).

In a reinjection scheme, one would like to site the reinjection wells as far away from producing zones and fractures as they may cause the reinjected colder water to move rapidly into the production zones causing an undesired thermal drawdown. However, as the distance from the production zones increases the likelihood of recharging the reservoir (and maintaining its pressure) decreases. A reinjection scheme must reconcile two contrasting requirements on the distance between the reinjection and production wells, namely the adequate pressure support from reinjection demands decreasing distance between wells, and the danger of thermal drawdown demands increasing it.

Thus, the design of reinjection scheme reduces to determining a safe distance between injection and production wells based on our understanding of the flow and heat transport characteristics of the reservoir being considered. The identification of major flow paths and estimation of major flow and heat transport parameters accurately, and hence, the design of reinjection schemes, continue to be major challenges for researchers and field operators (Stefansson, 1997, Axelsson *et al.*, 2001).

Kocabas (2004) has proposed that a joint the interwell tracer test with a thermal injection backflow test for estimating both hydrodynamic and thermal parameters, fast, reliable and in situ. The design of a thermal injection backflow test to estimate the heat transfer parameters with the least uncertainty is an important issue and should be explored in depth.

Estimation of parameter values from experimental data involves employment of a mathematical model through an inverse problem application. The most commonly employed method in inverse problems is the nonlinear regression analysis (Dogru et.al. 1977). In a regression analysis, usually one is interested in both the best estimate value of a parameter and how reliable that estimated value is. Furthermore, one would like to improve the reliability of the estimated parameters through a better design of laboratory and/or field experiments and sampling. The parameter sensitivity analysis has been the primary tool used to investigate abovementioned aspects of parameter estimation (Beck & Arnold 1977).

The sensitivity analysis is defined as the study of a system's responses to various disturbances whose central figure is the sensitivity coefficient (McElwee & Yukler 1978). The sensitivity coefficient is a partial derivative of the dependent variable of the model with respect to a parameter, and hence, represents the magnitude of the change in the dependent variable due to perturbations in the values of the parameters. For instance, the dimensionless temperature designated by T_D, is the dependent variable of the heat transport in porous media during nonisothermal injections. The dimensionless temperature is a function of dimensionless time, t_D, dimensionless distance, x_D, and a parameter vector α representing the physical processes included in the model.

Hence, the normalized sensitivity coefficient for a heat transport in fracture/ matrix configuration is defined as:

$$\chi_i = \alpha_i \frac{\partial T_D(x_D, t_D, \alpha)}{\partial \alpha_i} \quad (1)$$

Note that the normalized sensitivity coefficient is independent of the dimension and unit of a particular parameter (Jiao &Rushton 1995), thus allows one to compare the sensitivity to different parameters visually (McElwee 1987).

The functions of sensitivity coefficients in parameter estimation (Beck & Arnold 1977) are: (1) the uncertainty involved in the estimated values of the parameters is quantified via the sensitivity coefficients, (2) they function as the key figure of identifiability problem, (3) they allow optimal design of experiments where parameter estimation will be carried out.

The effect of sensitivity coefficient on the uncertainty of estimate will appear in the calculated confidence interval and variance. For a given confidence level, the width of the confidence interval is a measure of the uncertainty in the estimated parameter value (Knopman & Voss 1987). The larger the interval width the lesser the model sensitivity to that parameter, and hence, the more uncertainty in the estimated parameter value.

The identifiability is described as that the parameters can be better estimated if the sensitivity coefficients over the range of observations are linearly independent (Beck & Arnold 1977). The estimated parameter values will be nonunique if the sensitivity coefficients over the range of measurements are correlated or linearly dependent. Therefore, any combinations of parameters satisfying the linear dependency relation will equally produce the same observed profile. Hence, for models with multiple parameters, the normalized sensitivity coefficients should be plotted and examined for presence of a linear dependence. The linear dependence can be approximately verified by graphically adding the normalized sensitivities to obtain a zero for each observation point.

In an inverse problem, the uncertainty of each parameter estimate is related to the sensitivity of the model to that parameter and the measurement errors. First of all, if the variance in random error in observations is sufficiently large, then sensitivities can be obscured by that noise and the estimated parameters will have limited value. Considering reasonable measurement errors, the parameters can be best estimated if the absolute values of sensitivity coefficients are as large as possible and changing with time as well. Therefore, it makes little sense to try to determine a parameter if model sensitivity is low (Knopman & Voss 1987). In addition, if the model sensitivity reaches to constant value additional measurements will contribute little to reduce the uncertainty in the parameter estimate.

Owing to above facts, that information about a physical parameter can be most accurately obtained at points in space and time with high sensitivity to model parameters (McElwee, 1987. Therefore, sensitivity coefficients are used to determine those parts of spatial and temporal domains where model sensitivity to a parameter is highest. In other words, sensitivity coefficients are used to identify the most informative observation interval in time and observation point in space to refine the estimates of parameters. In addition, specifying the values of decision variables which lead to high sensitivity coefficients is another important objective. Achieving these two objectives are considered as the optimal design of experiments.

The optimal design and interpretation of a thermal injection backflow test through a novel mathematical model and its parametric sensitivity analysis form the main objective of this work and will be detailed below.

2. INJECTION BACKFLOW TESTS

During a thermal injection backflow testing a tracer may also be used investigate hydrodynamic characteristics of nearby area of the test well. A low temperature water is used as the tracer carrier as well as the driving fluid. First, a tracer slug is introduced into the water injected into the reservoir. This is followed by a continuous injection of low temperature water. When the predetermined injection time is reached the injection well is backflowed at the same rate or a different flow rate. During the backflow period, both feed-zone temperatures and the tracer concentrations in the backflowed fluid are recorded. After the temperatures of the produced fluid approach the preinjection reservoir temperature and an adequate amount of injected tracer is recovered, the backflow (i.e. production) of the injection well is stopped.

While the tracer return profiles are interpreted for estimating the hydrodynamic parameters, the temperature recovery profile is used to estimate the thermal parameters controlling the heat transfer in the system. This constitutes the procedure of the joint tracer and thermal injection backflow test application.

3. MATHEMATICAL MODELING

This work employs two conceptual models and both of them results in the same dimensionless mathematical models. The first model assumes a single vertical fracture of constant porosity, aperture, height, and the fracture is located in a low porosity rock matrix of infinite extent. The assumption of a flow through vertical fracture demands linear coordinate system; the flow velocity is constant within the fracture and the fluid in the matrix is virtually immobile. The injected low temperature water travels through the fracture and warms up due to heat transfer from adjacent matrix. The temperatures across the fracture are uniform and water and rock within the fracture and the matrix as well are in thermal equilibrium. The second model assumes a constant thickness reservoir of uniform porosity and permeability and a radial flow geometry extending from the wellbore far into the reservoir. The reservoir is confined by two impermeable layers of infinite extend. The temperature across the reservoir thickness is uniform and heat is transferred to/from the confining layers by conduction. The water and rock within the reservoir and the confining layers are in thermal equilibrium. While the first system is suitable for fractured geothermal reservoirs (Kocabas and Horne, 1990), the second system represents a sensible energy storage aquifer (Sauty et. al.1978 and Sauty et. al. 1982). The fracture/matrix system in a geothermal reservoir is the conceptual model employed in the following mathematical developments. The governing equations of heat flow in a sensible energy storage reservoir are presented in appendix A. The heat is a special type tracer, and hence, the governing differential equations of temperature transients are identical to that of tracer transients. Only the injection modes are different as we usually employ an instantaneous injection of a tracer slug called instantaneous injection whereas a continuous injection of a constant temperature fluid referred to as continuous injection. Therefore, the solutions for

thermal transients may be employed for tracer transients with slight modifications.

There is only a limited number of analytical solutions available for models of tracer injection backflow tests (Kocabas and Horne, 1987; Falade et al., 1987; and Falade and Brigham, 1989) or thermal injection backflow tests (Kocabas and Horne, 1990, and Kocabas, 2004). Among these models, the one which specifically considers the previously described fracture/matrix system is used by Kocabas and Horne (1987) for tracer flow, and Kocabas and Horne (1990) and Kocabas (2004) for heat flow in an injection backflow test. In both cases, an equal injection backflow flow rate is assumed, a double Laplace transform with respect to injection and backflow times is applied to obtain the solution in Laplace space and real space solution is also presented. A Laplace space solution has been presented for unequal injection and backflow rates (Kocabas, 1995) but left uninverted into the real space and the values were computed using a double numerical inversion technique. The equal flow solutions indicated that there is a large amount of numerical errors in the double numerical inversion specially in case of hyperbolic equations when Stehfest algorithm is used. This work employs the iterated Laplace transform technique to present a novel real space solution for unequal injection and backflow flow rates and the technique is detailed in the following.

2.1 Model Development for Thermal Injection Backflow Tests

Within that fracture/matrix geological configuration, while heat conduction in the flow direction is neglected, an infinite lateral thermal conductivity in the fracture and a constant thermal conductivity in the matrix are assumed. Thus, the governing equations become:

$$\rho_r c_r \frac{\partial T}{\partial t} + \rho_w c_w \phi u \frac{\partial T}{\partial x} - \frac{k_m}{b} \frac{\partial T_m}{\partial z} \Big]_{z=0} = 0 \qquad (2)$$

$$\rho_m c_m \frac{\partial T_m}{\partial t} - k_m \frac{\partial^2 T_m}{\partial z^2} = 0 \qquad (3)$$

The initial and boundary conditions are:

$$T = T_m = T_0 \quad \text{at} \quad t = 0 \qquad (4)$$

$$T = T_i \quad \text{at} \quad x = 0 \qquad (5)$$

$$T_m = T \quad \text{at} \quad z = 0 \qquad (6)$$

$$T_m \to 0 \quad \text{as} \quad z \to \infty \qquad (7)$$

To simplify the mathematical formulation the following dimensionless variables are used.

$$T_D = \frac{T_o - T}{T_o - T_i}, \quad T_{mD} = \frac{T_o - T_m}{T_o - T_i} \qquad (8)$$

$$x_D = \frac{k_m x}{\rho_w c_w \phi b^2 u}, \quad t_D = \frac{k_m t}{\rho_r c_r b^2} \qquad (9)$$

$$z_D = \frac{z}{b}, \quad \text{and} \quad \theta = \frac{\rho_m c_m}{\rho_r c_r} \qquad (10)$$

Using the above dimensionless variables yields:

$$\frac{\partial T_D}{\partial t_D} + \frac{\partial T_D}{\partial x_D} - \frac{\partial T_{mD}}{\partial z_D} \Big]_{z_D=0} = 0 \qquad (11)$$

$$\theta \frac{\partial T_{mD}}{\partial t_D} - \frac{\partial^2 T_{mD}}{\partial z_D^2} = 0 \qquad (12)$$

The dimensionless initial and boundary conditions become:

$$T_D = T_{mD} = 0 \quad \text{at} \quad t_D = 0 \qquad (13)$$

$$T_D = 1 \quad \text{at} \quad x_D = 0 \qquad (14)$$

$$T_{mD} = T_D \quad \text{at} \quad z_D = 0 \qquad (15)$$

$$T_{mD} \to 0 \quad \text{as} \quad z_D \to \infty \qquad (16)$$

Using the Laplace transform, the following Laplace domain solutions of injection period are obtained (Kocabas, 2004):

$$\dot{T}_D = \frac{1}{s} \exp(-s x_D) \exp(-\sqrt{\theta s}\, x_D) \qquad (17)$$

$$\dot{T}_{mD} = \frac{\exp(-s x_D)}{s} \exp(-\sqrt{\theta s}\, x_D) \exp(-\sqrt{\theta s}\, z_D) \qquad (18)$$

For the backflow period the relevant governing equations must be solved treating the injection period solutions as the initial condition values.

During the backflow period, the governing equations change due to both the reversal in the flow direction and presence of a different backflowflow rate than that in injection period. Using t_p as the time variable for the backflow period, dimensionless governing equations for the backflow period are:

$$\frac{\partial T_D}{\partial t_{pD}} - \frac{1}{\lambda} \frac{\partial T_D}{\partial x_D} - \frac{\partial T_{mD}}{\partial z_D} \Big]_{z_D=0} = 0 \qquad (19)$$

$$\theta \frac{\partial T_{mD}}{\partial t_{pD}} - \frac{\partial^2 T_{mD}}{\partial z_D^2} = 0 \qquad (20)$$

Where the ratio of the injection rate to backflow rate and dimensionless backflow time are defined respectively as:

$$\lambda = \frac{u}{u_b} \qquad (21)$$

and

$$t_{pD} = \frac{k_m t_p}{\rho_r c_r b^2} \qquad (22)$$

The other dimensionless variables are defined by Equations 8, 9 and 10. The initial and boundary conditions for the backflow period are specified in Equations 23, 25 and 26:

$$T_D = T_D(t_{Di}, x_D) \quad \text{at} \quad t_{pD} = 0 \qquad (23)$$

Where t_i is the total injection time and, hence,

$$t_{Di} = \frac{k_m t_i}{\rho_r c_r b^2} \tag{24}$$

$$T_{mD} = T_{mD}(t_{Di}, x_D) \qquad \text{at} \qquad t_{pD} = 0 \tag{25}$$

$$T_D = 0 \qquad \text{at} \qquad x_D = x_{DL} = \frac{k_m (u t_i)}{\rho_w c_w \phi b^2 u} \tag{26}$$

The boundary conditions for the bounding layer remain unchanged, and hence, Equations 15 and 16 apply.

Using a second Laplace transform with respect to t_{pD}, one may arrive at the solution for the backflow period (Kocabas, 2004, also see Appendix B). Since the only point of observation during the backflow period is the injection well, the temperature recovery with time for the feed-zone in the injection well is given by:

$$\ddot{T}_D = \frac{1}{s}\left[1 + \frac{\sqrt{\theta}}{\sqrt{s}+\sqrt{p}}\right]\left[\frac{\lambda}{s + \sqrt{\theta s} + \lambda p + \lambda\sqrt{\theta p}}\right] \tag{27}$$

The real space solution given by Eq. 28, has been obtained by applying the technique of iterated Laplace transform to Eq. 27. The iterated Laplace transform (Sneddon, 1972) is an easy yet highly powerful technique to invert significantly complicated Laplace space equations. Note for a unit λ value, Eq. 28 reduces to the previously presented to solution (Kocabas, 2004) for the equal injection and backflow rates.

$$T = \int_0^{\min(1,\frac{t_n}{\lambda})} \left(\frac{\lambda^2\sqrt{\alpha}\,\tau}{2(t_n - \lambda\tau)} + \lambda\sqrt{\alpha}\right) G(\tau)\, d\tau + \int_0^1 d\eta \int_0^{\min(1-\eta,\frac{t_n+\eta}{\lambda})} \left(\frac{\lambda^2\alpha\tau}{t_n + \eta - \lambda\tau} - \frac{\lambda\alpha\tau}{1-\eta-\tau}\right) F(\eta) d\tau \tag{28}$$

where

$$G(\tau) = \frac{\exp\left(-\frac{\lambda^2\alpha\tau^2}{4(t_n - \lambda\tau)}\right)}{\sqrt{\pi(t_n - \lambda\tau)}} \; erfc\left(\frac{\sqrt{\alpha\tau}}{2\sqrt{(1-\tau)}}\right) \tag{29}$$

$$F(\eta) = \frac{\exp\left(\frac{-\alpha\tau^2}{4(1-\eta-\tau)}\right)}{2\sqrt{\pi(1-\eta-\tau)}} \; \frac{\exp\left(\frac{-\lambda^2\alpha\tau^2}{4(t_n+\eta-\lambda\tau)}\right)}{2\sqrt{\pi(t_n+\eta-\lambda\tau)}} \tag{30}$$

$$\alpha = \theta t_{Di} \tag{31}$$

2.2 Designing Thermal Injection Backflow Tests and Estimation of Thermal Parameters

Equations 28 through 31 show that the temperature recovery profile is a function of three operational variables and a model parameter group designated by α. The operational parameters are the temperature difference between the injected fluid and reservoir temperatures, the total injection time, t_i, and the ratio of injection flow rate to backflow rate, λ. The design of a thermal injection backflow test requires us to select the combination of three operational (decision) variables so that the model parameter λ have the highest sensitivity coefficient in the measurement domain of backflow period.

The parameter group $\alpha = \theta t_{Di}$, represents the collective role of a number of parameters. In order to investigate the influence of the product θt_{Di} , first a thermal characteristic time, t_{th}, is defined:

$$t_{th} = \frac{\rho_r c_r b^2}{k_m} \tag{32}$$

Then, the product θt_{Di} can be written as:

$$\theta t_{Di} = \frac{\rho_m c_m}{\rho_r c_r}\frac{k_m t_i}{\rho_r c_r b^2} = \theta\frac{t_i}{t_{th}} \tag{33}$$

In Eq. 33, the parameter θ represents the ratio of the heat storage capacity of the confining matrix to that of the fracture. The characteristic time for heat transport from the matrix to the fracture zone is represented by t_{th} which is a strong function of fracture width and , t_i is the total injection time. One can deduce that the heat extraction/addition from/to the injected fluid depends directly on θ and total injection time, and inversely on the characteristic time t_{th}.

By using a nonlinear regression technique we can match temperature recovery profile from a thermal injection backflow test to a mathematical curve described by Eq. 28 and obtain an estimate of the only model parameter product $\alpha = \theta t_{Di}$. Once the parameter is estimated, we can readily calculate the product θ/tth from Eq. 33 as ti is the total injection time.

The first objective in our design is identifying the most informative observation interval of backflow time domain for the physical parameter α which will be estimated. The normalized sensitivity coefficient of α must be plotted to identify the interval of backflow time domains where model sensitivity to the parameter α is highest. In practice, the most informative interval of a domain and most informative values of decision variables are those which result in the highest absolute normalized parametric sensitivities. Also note that a high but constant sensitivity domain is less informative than that where the normalized sensitivity is varying. In other words, if there is a region with high sensitivity but the normalized sensitivity does not vary any additional measurement in this range will not contribute to the information about the parameter of interest.

The second objective is to select values of the operational variables (the decision variables of an engineering design) such that the sensitivity coefficient of α is highest in the measurement domain. In addition, considering the uncertainty of a parameter estimate is related to the sensitivity of the model to that parameter and the measurement errors, if the variance in random error in observations is sufficiently large, then sensitivities can be obscured by that noise. Thus, setting decision variable values such that measurement errors will be minimized is the other half of the second objective of design.

Thus design of an injection backflow test using the fracture/matrix model requires us specify the most informative values of operational variables, the time domain to sample and the required frequency of sampling so that model parameter α is estimated with the least uncertainty.

The abovementioned design aspects of thermal injection backflow tests are illustrated in the following.

Fig. 1 shows the dimensionless temperature return profiles for a typical $\alpha=\theta t_{Di}$ value of 0.1 and a range of ratios of injection rate to backflow rate, namely λ values. The figure show that if the value of the parameter λ is greater than 1 then the sampling domain increases without significant loss of information.

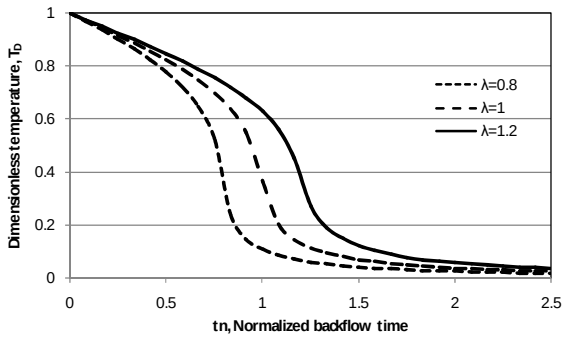

Figure 1: Variation of sampling domain with various ratios of injection rate to backflow rate, λ, and for α=0.1.

Fig. 2 shows that normalized sensitivities to α, for various λ values all have similar values in magnitude. It also show that sensitivity profile is varying significantly over the normalized time domain. However, the greatest time range where sensitivity profile is varying belongs to the curve of λ=1.2. Therefore, the figure shows that a slower backflow rate will allow more sampling data with less uncertainty in the estimates.

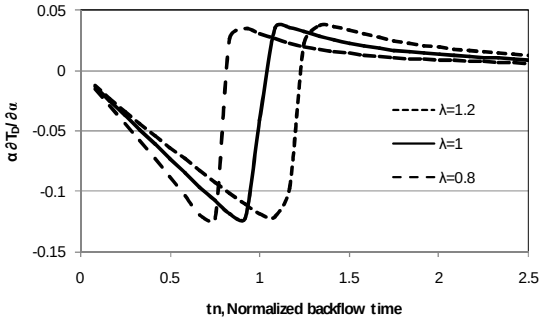

Figure 2: Normalized sensitivity profiles of α for various λ values and at α = θtDi=0.1

Fig.3 show the normalized sensitivities to α, for various α values and for a fixed value of λ=1.2. All curves show that sensitivities vary over the measurement domain. However, the greatest absolute sensitivity values belong to α values less than 1. This means that as the α values become greater than 1 the uncertainty in the estimates will increase.

The value of the parameter α increases with increasing θ/t_{th} and/or increasing total injection time. There arise the dilemma of injection backflow design. To be able to investigate a larger distance into the reservoir one should keep total injection time as high as possible. On the other hand, increasing injection time reduces the sensitivity of the estimated parameter which leads to estimates with less confidence.

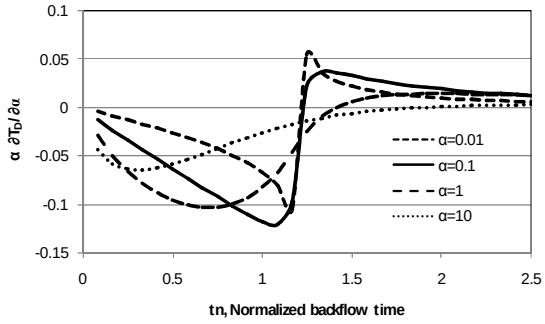

Figure 3: The Normalized sensitivity profiles of α for various α values and at λ= 1.2.

In order to resolve this issue one should take a closer look into the sensitivity of α=10 exhibited in Fig.4. Fig. 4 show that the normalized sensitivity to α do in fact vary significantly. However, the absolute value of sensitivity values are significantly smaller than those of α less than 1. In this case, to be able to estimate the parameter one should minimize the magnitude of measurement errors relative to the measured temperatures. This requires that one needs to increase the difference between the injected fluid temperature and the original reservoir temperature. In such a case, even the small variations in normalized temperatures will be distinguishable in actual temperature values.

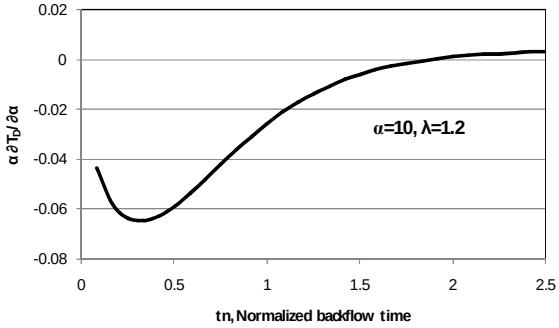

Figure 4: Normalized sensitivity profile of α for α=10 and λ=1.2

Thus the design reduces to balancing between the desired total injection time and the difference between the injected fluid and original reservoir temperatures.

Finally, Figures 3 and 4 show that the sampling frequency should be maximum around a normalized time of 1 for α values equal to 1 or less. On the other hand, the sampling frequency must be increased at much earlier backflow times for significantly greater than 1. The high frequency is required to capture the greatest variation zone of the sensitivities which contains the most reliable information about the physical parameter.

CONCLUSIONS

Novel solutions to a thermal injection backflow test in a fractured geothermal reservoir and in a sensible energy storage aquifer have been developed to estimate heat transport parameters in situ. The new analytical model of the thermal injection backflow test presented provides valuable insight into the collective roles of parameters controlling heat transport in a single vertical fracture or a radial flow of heat in a sensible energy storage reservoir.

The double Laplace transform technique is used to develop the Laplace space solutions of governing equations. Then, the Laplace space solutions were inverted into real space using the powerful technique of iterated Laplace transform.

The developed solutions are employed in a parametric sensitivity analysis to design the field test. The sensitivity analysis showed that a slower backflow is more informative. Hence, the decision variable of injection to backflow ratio should be specified as greater than 1 somewhere close to 1.2.

The total injection time as a second decision variable must be balanced between the requirement of a larger distance of investigation and lower sensitivity of return profiles which means more uncertainty in the estimated values. This shortcoming can be overcome by controlling the third decision variable namely the difference between the injected fluid and original reservoir temperature.

Finally the sampling frequency requirement over the time domain has been specified based on the expected value of the model parameter α.

It is also shown that the proposed testing procedure based on a parametric sensitivity analysis reduces the uncertainty in the parameter estimates greatly.

Consequently, the presented design procedure and the new interpretation models will help the operators to improve the design of injection backflow tests, and hence, reinjection schemes.

NOMENCLATURE

b = half fracture width, m

c_m = specific heat of the matrix, J/kg.^{o}C

c_r = specific heat of fracture bulk material, J/kg.^{o}C

c_s = specific heat of reservoir rock, J/kg.^{o}C

c_w = specific heat of geothermal water, J/kg.^{o}C

k_m = thermal conductivity of the matrix, W/m.^{o}C

x = distance along flow direction, m

x_D = dimensionless distance along flow direction

x_{DL} = dimensionless distance of convective front at total injection time

T = temperature in the fracture, .^{o}C

T_i = temperature of the injected fluid, .^{o}C

T_0 = initial reservoir temperature, .^{o}C

T_D = dimensionless temperature of fracture

T_m = temperature of the matrix, .^{o}C

T_{mD} = dimensionless temperature of matrix

t_D = dimensionless time

t_{Di} = dimensionless total injection time

t_d = characteristic time for dispersive transport, hr

t_i = total injection time, hr

t_n = backflow period time normalized by total injection time, $_{tp}/t_i$

t_p = time variable during backflow period, hr

t_{pD} = dimensionless time during backflow period

t_{th} = thermal characteristic time, hr

s = Laplace transform variable of injection time.

p = Lapace transform variable of backflow time.

q = injection rate, m^3/hr

u = interstitial flow velocity, m/hr

z = distance normal to flow direction, m

z_D = dimensionless distance normal to flow direction

θ = ratio of the heat storage capacity of matrix to that of fracture

τ = convolution variable

η = dummy variable

ϕ = fracture porosity

ϕ_m = matrix porosity

ρ_m = bulk density of the matrix, kg/m^3

ρ_r = bulk density of the fracture, kg/m^3

ρ_s = density of the reservoir rock, kg/m^3

ρ_w = density of the geothermal water, kg/m^3

REFERENCES

Axelsson, G., Flovenz, O. G., Hauksdottir, S., Hjartarson, A., and Liu, J., 2001. Analysis of tracer test data and injection induced cooling, in the Laugaland geothermal field, N-Iceland, Geothermics, 30, pp. 697-725.

Beck, J.V. & Arnold, K.J. 1977. Parameter Estimation in Engineering and sciences. New York. John Wiley and Sons.

Dogru, A.H., Dixon, T.N., & Edgar, T.F., Confidence limits on the parameters and predictions of slightly compressible single phase reservoirs; Soc. Pet. Eng. J., pp. 42-56, Feb 1977

Ditkin, V. A. and Prudnikov, A. P., 1962. *Operational Calculus in Two Variables*, Int. Series Pure Appl. Math., Pergamon Press, London, pp. 46-47.

Falade, G.K., Antunez, E., and Brigham, W.E., 1987. Mathematical analysis of single-well tracer tests, Tecnical Report Supri Tr-57, Stanford University Petroleum Research Institute, Stanford, CA.

Falade, G.K. and Brigham W.E., Feb. 1989. Analysis of radial transport of reactive tracer in Porous media," SPE#16033, SPE Reservoir Engineering, pp. 85-90.

Jiao, J. J. & Rushton, K. R. 1995. Sensitivity of drawdown to parameters and its influence on parameter estimation for pumping tests in large diameter wells. Ground water v. 33, No. 5:794-800

McElwee, C. D. 1987. Sensitivity analysis of groundwater models. In J. Bear & M. Y. Corapcioglu (eds), Advances in Transport Phenomena in Porous Media 750-817. Dordrecht. Martinus Nijhoff Publishers.

McElwee, C.D. & Yukler, M. A. 1978. Sensitivity of groundwater models with respect to variations in transmissivity and storage. Water Resources Research vol:13 no:3:451-459.

Knopman, D. S. & Clifford, I. Voss. 1987. Behavior of Sensitivities in the one-diemensional advection-dispersion equation: Implications for parameter estimation and sampling design. Water Resources Research vol:23 no:2:253-272.

Kocabas, I. 2005. Geothermal reservoir characterization via thermal injection-backflow and interwell tracer testing, Geothermics 34 , pp. 27-46.

Kocabas, I. 1995. Using interwell test data to determine the interaction between geological structure and reinjection processes in geothermal reservoirs, Proceedings, International Earth Sciences Colloquim on the Aegean Region, Izmir-Gulluk, Turkey, pp. 739-751.

Kocabas, I. and Horne, R. N., 1987. Analysis of injection-backflow tracer tests in fractured geothermal reservoirs, Proceedings, Twelfth Workshop on Geothermal Engineering, Stanford Univ., Stanford, CA, pp. 233-240.

Kocabas, I. and Horne, R. N., 1990. A new method of forecasting the thermal breakthrough time during reinjection in geothermal reservoirs, Proceedings, Fifteenth Workshop on Geothermal Engineering, Stanford Univ., Stanford, CA, pp. 179-186.

Sauty, J. P, Gringarten, A., Landel, P.A., 1978. The effect of thermal dispersion on injection of hot water in aquifers. Proc. The Second Invitational Well Testing Symposium, Div. Of Geothermal Energy, U.S. Dept. of Energy. Berkeley CA., pp. 122-131

Sauty, J. P., Gringarten, A., Menjoz, A. and Landel, P.A., 1982. Sensible energy storage in aquifers: 1. Theoretical study, water resources research, Vol. 18 (2), pp.245-252.

Sneddon,, I.A., The use of integral Transforms, MCGRaw Hill, NY, 1972

Stefansson, V., 1997. Geothermal reinjection experience, Geothermics, 26(1), pp. 99-139.

Voelker, D. and Doetsch, G., 1950. *Die Zweidimensionale Laplace-Transformation,* Birkhauser, Basel Switzerland, pp.186-187.

APPENDIX A: DERIVATION OF GOVERNING EQUATIONS FOR RADIAL FLOW

Within that reservoir confined by impermeable cap and base rocks configuration, while heat dispersion in the flow direction is neglected, an infinite vertical thermal conductivity in the reservoir and a constant thermal conductivity in the confining layers are assumed. Thus, the governing equations become:

$$\rho_r c_r \frac{\partial T}{\partial t} + \frac{\rho_w c_w q}{2\pi r h}\frac{\partial T}{\partial x} - \frac{2k_m}{h}\frac{\partial T_m}{\partial z}\Big]_{z=0} = 0 \quad \text{(A.1)}$$

$$\rho_m c_m \frac{\partial T_m}{\partial t} - k_m \frac{\partial^2 T_m}{\partial z^2} = 0 \quad \text{(A.2)}$$

The initial and boundary conditions are specified as the same as those given by Eq. 4 through 7 except, Eq. 5. The radial inner boundary condition is specified follows

$$T = T_i \qquad \text{at} \qquad r = 0 \quad \text{(A.3)}$$

While the dimensionless temperatures are defined by Eq. 8, the dimensionless variables are defined as follows:

$$r_D = \frac{4k_m \pi r^2}{\rho_w c_w h q}, \quad t_D = \frac{4k_m t}{\rho_r c_r h^2} \quad \text{(A.4)}$$

$$z_D = \frac{2z}{h}, \qquad \text{and} \qquad \theta = \frac{\rho_m c_m}{\rho_r c_r} \quad \text{(A.5)}$$

Using the above defined dimensionless variables one obtains:

$$\frac{\partial T_D}{\partial t_D} + \frac{\partial T_D}{\partial r_D} - \frac{\partial T_{mD}}{\partial z_D}\Big]_{z_D=0} = 0 \quad \text{(A.6)}$$

$$\theta \frac{\partial T_{mD}}{\partial t_D} - \frac{\partial^2 T_{mD}}{\partial z_D^2} = 0 \quad \text{(A.7)}$$

(A.6) and (A.7) are of the same form of Eq. 11 and Eq. 12. The dimensionless initial and boundary conditions also become the same as those Eq. 13 through 16 except, eq. 14. The inner boundary condition in dimensionless form becomes:

$$T_D = 1 \qquad \text{at} \qquad r_D = 0 \quad \text{(A.8)}$$

Thus the solution of Eq. 11 and Eq. 12 are also the solution of radial flow systems for the considered models in this work.

APPENDIX B: DERIVATION OF THE REAL SPACE TEMPERATURE RECOVERY PROFILE FOR A THERMAL INJECTION BACKFLOW TEST

Applying a double Laplace transform (Ditkin and Prudnikov, 1962) with respect to the dimensionless variables t_{Di} and t_{pD} to the dimensionless backflow equations and their initial and boundary conditions (equations 19 through 26), yields the double Laplace transformed solution of the fracture equation, Eq. 19, given by (B.1):

$$\ddot{T}_D = \ddot{T}_{x_D=0}\begin{Bmatrix} \exp(-sx_D)\exp(-\sqrt{\theta s}\, x_D) - \\ \exp(-sx_{DL})\exp(\sqrt{\theta s}\, x_{DL}) \\ \exp[-\lambda p(x_{DL} - x_D)] \\ \exp[-\lambda\sqrt{\theta_1 p}(x_{DL} - x_D)] \end{Bmatrix} \quad \text{(B.1)}$$

where

$$\ddot{T}_{x_D=0} = \left[\frac{1}{s} + \frac{\sqrt{\theta}}{s+s\sqrt{p}}\right] \frac{\lambda}{s+\sqrt{\theta s}+\lambda p+\lambda\sqrt{\theta p}} \quad \text{(B.2)}$$

Since we can only measure the temperatures at the well (i.e. $x_D = 0$), the solution (B.1) at $x_D = 0$ may be expressed as:

$$\ddot{T}_D = \ddot{F}(s,p,\theta) - \ddot{G}(s,p,\theta) \exp(-x_{DL}s)\ \exp(-\lambda x_{DL}p) \quad \text{(B. 3)}$$

In real space, (B.3) will have the form :

$$T_D = F(t_{Di}, t_{pD}, \theta) - G(t_{Di}-x_{DL}, t_{pD}-\lambda x_{DL}, \theta)\, H(t_{Di}-x_{DL}, t_{pD}-\lambda x_{DL}) \quad \text{(B. 4)}$$

Where H is the Heaviside step function.

Since during the injection period the farthest distance traveled by the injected fluid is equal to ut_i, using Equations 24 and 26, we can show:

$$\frac{t_{Di}}{x_{DL}} = \frac{\phi\rho_w c_w}{\phi\rho_w c_w + (1-\phi)\rho_s c_s} \le 1 \quad \text{(B.5)}$$

Since, according to Eq. (B.5) $t_{Di} \le x_{DL}$ the Heaviside step function and as a result the second term of Eq. (B.4) will always be zero. Therefore, the nonzero part of the solution will be the inverse of only (B.2).

To obtain a real space solution, we rewrite (B.2) as:

$$\ddot{T}_D = \left[\frac{1}{s} + \frac{\sqrt{\theta}}{s\sqrt{p}} + \frac{\sqrt{\theta}}{(s-p)}\left(\frac{1}{\sqrt{s}} - \frac{1}{\sqrt{p}}\right)\right] \left[\frac{\lambda}{s+\sqrt{\theta s}+\lambda p+\lambda\sqrt{\theta p}}\right] \quad \text{(B.6)}$$

In order to invert (B.6), we employ the method of iterated Laplace transform. In order to proceed let's first divide (B.6) into three parts, namely each part within the left square brackets multiplied by that in the right square brackets and call them T_{D1}, T_{D2} and T_{D3}. Then, iterative Laplace transform inversion is applied to each term separately.

For T_{D1}, the first iteration of Laplace inversion is applied to the s in the denominator of the term in right square brackets to obtain:

$$L_1^{-1}\ddot{T}_{D1} = L_1^{-1}\frac{1}{s}\frac{\lambda}{s+\sqrt{\theta s}+\lambda p+\lambda\sqrt{\theta p}} = \frac{\lambda}{s}\exp(-\sqrt{\theta s}\tau)\exp(-\lambda p\tau)\exp(-\lambda\sqrt{\theta p}\tau) \quad \text{(B.7)}$$

The second iteration is applied to the remaining s terms in (B.7) to obtain:

$$L_2^{-1}\frac{\lambda}{s}\exp(-\sqrt{\theta s}\tau) = erfc\left(\frac{\sqrt{\theta}\tau}{2\sqrt{t_{Di}-\tau}}\right) \quad \text{(A. 8)}$$

Since the inversion is applied iteratively, the final result must be convolution of the results of the two steps, yielding:

$$L^{-1}\ddot{T}_{D1} = \dot{T}_{D1} = \int_0^{t_{Di}} \lambda erfc\left(\frac{\sqrt{\theta}\tau}{2\sqrt{t_{Di}-\tau}}\right) \exp(-\lambda p\tau)\exp(-\lambda\sqrt{\theta p}\tau)\,d\tau \quad \text{(B.9)}$$

Inversion of exponential function in (B.9) with respect to Laplace variable p results in:

$$L^{-1}\begin{pmatrix}\exp(-\lambda p\tau)\\ \exp(-\lambda\sqrt{\theta p}\tau)\end{pmatrix} = H\left(t_{pD}-\lambda\tau\right) erfc\left(\frac{\lambda\sqrt{\theta}\tau}{2\sqrt{t_{pD}-\lambda\tau}}\right) \quad \text{(B.10)}$$

Thus, the double Laplace inversion of T_{D1} becomes:

$$T_{D1} = \int_0^{\min(t_{Di}, \frac{t_{Dp}}{\lambda})} \left\{ erfc\left(\frac{\sqrt{\theta}\tau}{2\sqrt{t_{Di}-\tau}}\right) \frac{\lambda^2\sqrt{\theta}\tau}{2\sqrt{(t_{pD}-\lambda\tau)^3}} \exp\left(\frac{-\lambda^2\theta\tau^2}{4(t_{pD}-\lambda\tau)}\right)\right\} d\tau \quad \text{(B.11)}$$

Similarly, first the iterated Laplace inversion and then the double Laplace inversion of T_{D2} can be obtained. For the third term, however, we the utilize the following operational relation [Voelker, 1950]

$$\frac{1}{s-p} f(s,p) = \int_0^{t_{Di}} F(t_{Di}-\eta, \tau_D+\eta)\, d\eta \quad \text{(B.12)}$$

and the iterated and double Laplace transform inversions are sequencially applied to the part of the third term which remains after excluding 1/(s-p) term. Finally, the real space solution becomes:

$$T = \int_0^{\min(t_{Di}, \frac{t_{pD}}{\lambda})} \left(\lambda\sqrt{\theta} + \frac{\lambda\sqrt{\theta}\,\tau}{2(t_{pD}-\lambda\tau)}\right) G(\tau)\,d\tau + \int_0^{t_{Di}} d\eta \int_0^{\min(t_{Di}-\eta, \frac{t_{pD}+\eta}{\lambda})} \left(\frac{\lambda^2\sqrt{\theta}\,\omega}{\tau_D+\eta-\lambda\tau} - \frac{\lambda\sqrt{\theta}\,\tau}{t_{Di}-\eta-\tau}\right) F(\eta)\,d\tau \quad \text{(B.13)}$$

Where

$$G(\tau)=\left\{\begin{array}{c}\dfrac{\exp\left(-\dfrac{\lambda^2\theta\tau^2}{4(\tau_D-\lambda\tau)}\right)}{\sqrt{\pi(t_{pD}-\lambda\tau)}}\\ erfc\left(\dfrac{\sqrt{\theta}\tau}{2\sqrt{(t_{Di}-\tau)}}\right)\end{array}\right\} \qquad \text{(B.14)}$$

$$F(\eta)=\left\{\begin{array}{c}\dfrac{\exp\left(-\dfrac{\lambda^2\theta\tau^2}{4(t_{Di}-\eta-\tau)}\right)}{2\sqrt{\pi(t_{Di}-\eta-\tau)}}\\ \dfrac{\exp\left(-\dfrac{\lambda^2\theta\tau^2}{4(t_{pD}+\eta-\lambda\tau)}\right)}{\sqrt{\pi(t_{pD}+\eta-\lambda\tau)}}\end{array}\right\} \qquad \text{(B.15)}$$

Normalizing all variables by t_{Di}, and setting the normalized backflow time t_n as:

$$t_n=\frac{t_i}{t_p}, \qquad \text{(B.16)}$$

we obtain Eq. 33.